

Magnetic impurities and itinerant carriers in doped SrTiO₃: Anomalous Hall resistivity

D. Satoh,¹ K. Okamoto,¹ and T. Katsufuji^{1,2,3,*}

¹*Department of Physics, Waseda University, Tokyo 169-8555, Japan*

²*Kagami Memorial Laboratory for Material Science and Technology, Waseda University, Tokyo 169-0051, Japan*

³*PRESTO, Japan Science and Technology Agency, Saitama 332-0012, Japan*

(Received 12 December 2007; revised manuscript received 8 February 2008; published 6 March 2008)

We studied perovskite SrTiO₃ into which magnetic impurities (Cr or V) and itinerant carriers (electrons in the Ti 3*d* band) are introduced. We found that the itinerancy of the electrons on the magnetic impurities and magnetic properties of the compounds depend on the species of the transition metal as impurities. Anomalous Hall resistivity was observed in Cr-doped SrTiO₃, and it was found that its coefficient is inversely proportional to the number of itinerant carriers.

DOI: [10.1103/PhysRevB.77.121201](https://doi.org/10.1103/PhysRevB.77.121201)

PACS number(s): 72.20.My, 71.28.+d, 75.20.Hr, 75.50.Pp

How magnetic impurities behave in the sea of itinerant carriers has been an important subject of condensed matter physics. Various kinds of phenomena, for example, Kondo effect, exotic magnetism, negative magnetoresistance, and anomalous Hall effect, are dominated by the coupling between magnetic impurities and itinerant carriers.¹ Recently, dilute magnetic semiconductors have been extensively studied based on GaAs,² and physics of magnetic impurities and itinerant carriers is important also in those compounds. There are several parameters to characterize such a system; the transfer energy of itinerant carriers, the transfer matrix of mixing between the localized states at the magnetic impurity and the extended states of the itinerant carriers, and the Coulomb repulsion energy appearing when an additional electron is added to the magnetic impurity. One basic question about this kind of system is whether the localized electrons on the magnetic impurities become itinerant or not by the hybridization with the extended states. In relation to this question, magnetic properties dominated by the magnetic interaction via itinerant carriers are also important issues and are characterized by the competition between Kondo effect favoring a spin-singlet state and Ruderman-Kittel-Kasuya-Yosida (RKKY) interaction favoring a magnetically ordered state.

Perovskite SrTiO₃ is a parent material suitable to introduce both magnetic impurities and itinerant carriers.^{3,4} In this compound, Ti ions occupy the *B* site of the perovskite structure (ABO₃) forming the ideal cubic lattice and are 4+, where there is no electron in the *d* state. When Sr²⁺ at the *A* site of the perovskite structure is substituted by La³⁺, an electron is introduced to the *d* state of Ti, nominally represented as Ti³⁺, and this electron acts as an itinerant carrier in the *d* band.⁵ Furthermore, the Ti ion at the *B* site can be substituted by other transition metals, such as V and Cr, and those act as magnetic impurities. It is unique in this series of compounds that both itinerant carriers and electrons on the magnetic impurity are in the same *d* orbital, which is quite different from other systems, where they usually exist in different types of orbitals.

In this Rapid Communication, we report the transport and magnetic properties of SrTiO₃ with the substitution of La by Sr and Ti by Cr or V to clarify how magnetic impurities behave in the sea of itinerant carriers. We found that various characteristics, for example, whether the electrons on the

magnetic impurities are localized or delocalized, and whether the system is magnetic or nonmagnetic, strongly depend on the species of the transition metal as magnetic impurities. We also found that this series of compounds gives us unique opportunities to study the physics of anomalous Hall effect.

Samples of Sr_{1-x-y}La_{x+y}Ti_{1-x}V_xO₃ were synthesized by the floating-zone technique in the flow of 7% H₂ gas, similar to the technique previously used to make Sr_{1-x}La_xTiO₃.⁵ We tried to make Sr_{1-x-y}La_{x+y}Ti_{1-x}Cr_xO₃ in a similar way, but found that homogeneous samples cannot be obtained over a wide range of *x* and *y*. Thus, we employed a different technique; appropriate amounts of oxides are mixed and pressed into a rod and sintered in the floating-zone furnace with the flow of 7% H₂ gas slightly below the melting point. We found that the samples of Sr_{1-x}La_xTiO₃ (without Cr) made by the same technique exhibit almost the same absolute values and temperature dependence of resistivity as that of the single crystal made by the floating-zone technique. This allows us to believe that the crystalline domain boundaries do not seriously affect the transport properties of the present polycrystalline Cr-doped samples. We performed thermogravimetric analysis of the samples and found that the number of oxygen is 3.00 ± 0.007. In the above notation of chemical composition, *x* represents the concentration of magnetic impurities and *y* the concentration of Ti³⁺ (nominal itinerant carriers), with the assumption that all the Cr or V ions are 3+. The configuration of the *d* electrons is summarized in Fig. 1(a). Resistivity and Hall measurements were performed by conventional four-probe technique, and magnetization was measured by a superconducting quantum interference device magnetometer. Reflectivity measurement was done for the melt-grown V-doped samples with a Fourier transform infrared spectrometer between 0.1 and 0.8 eV and a grating spectrometer between 0.7 and 5 eV.

A distinct difference between Cr and V as magnetic impurities is seen in the dependence of magnetic susceptibility (χ) on carrier concentration. In Fig. 2, data when the value of *x* (number Cr or V) is fixed to 0.2 and the value of *y* (number of Ti³⁺) is varied are shown. For *y*=0 [shown by the thick solid line in Figs. 2(a) and 2(b)], χ is enhanced with decreasing temperature (*T*) for both Cr and V. We fit the data by a Curie-Weiss law and found that the Curie moment estimated

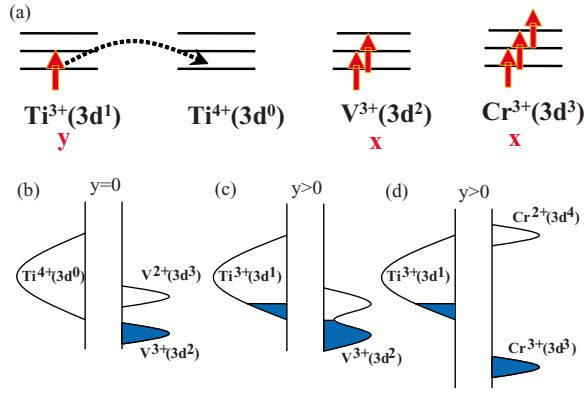


FIG. 1. (Color online) (a) Configuration of d electrons at each ion. [(b)–(d)] Schematic pictures of the electronic state of SrTiO_3 with V or Cr as impurities.

from the data above 100 K is $0.45 \text{ K cm}^3/\text{mol}$ for Cr and $0.21 \text{ K cm}^3/\text{mol}$ for V, consistent with the values when the $S=3/2$ (Cr) or $S=1$ (V) moment exists by 20% of the B site. Resistivity (ρ) at room temperature is about $\sim 10^3 \Omega \text{ cm}$ for Cr and $\sim 10^1 \Omega \text{ cm}$ for V (not shown). Note that the resistivity of LaCrO_3 and LaVO_3 at room temperature is about $3 \times 10^3 \Omega \text{ cm}$ (Ref. 6) and $1 \times 10^{-1} \Omega \text{ cm}$,⁷ respectively. These indicate that all the Cr and V ions are 3+ and behave as localized moments ($S=3/2$ for Cr^{3+} and $S=1$ for V^{3+}), whereas all the Ti ions are 4+ and there is no itinerant carrier

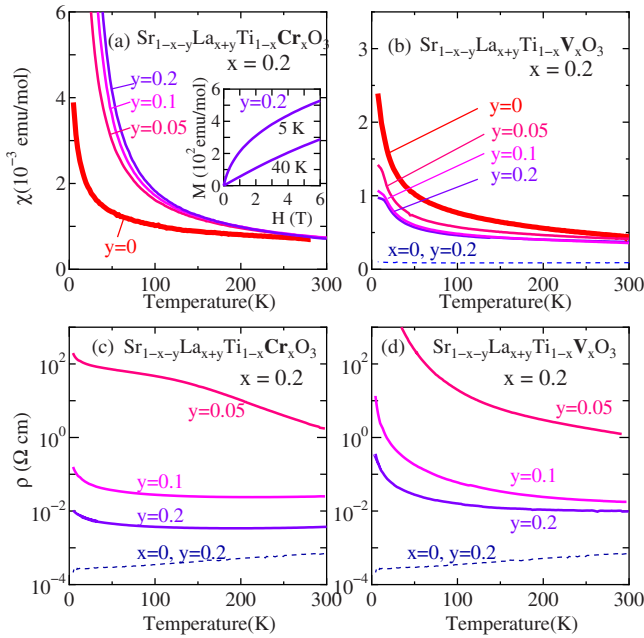


FIG. 2. (Color online) Upper panel: Temperature dependence of magnetic susceptibility of (a) $\text{Sr}_{1-x-y}\text{La}_{x+y}\text{Ti}_{1-x}\text{Cr}_x\text{O}_3$ and (b) $\text{Sr}_{1-x-y}\text{La}_{x+y}\text{Ti}_{1-x}\text{V}_x\text{O}_3$ with fixed Cr or V concentration, $x=0.2$, and various nominal concentrations of itinerant carriers (Ti^{3+}) y . The inset in (a) shows the magnetic-field dependence of magnetization for $y=0.2$. The dashed line in (b) is the data for $y=0.2$ without V or Cr. Lower panel: Temperature dependence of electrical resistivity of (c) $\text{Sr}_{1-x-y}\text{La}_{x+y}\text{Ti}_{1-x}\text{Cr}_x\text{O}_3$ and (d) $\text{Sr}_{1-x-y}\text{La}_{x+y}\text{Ti}_{1-x}\text{V}_x\text{O}_3$ with fixed x (number of Cr or V) and various values of y (number of Ti^{3+}). The dashed lines in (c) and (d) are the data without V or Cr.

(Ti^{3+}) for both Cr and V with $y=0$. On the other hand, when y is increased, resistivity decreases down to $10^{-2} \Omega \text{ cm}$ for both Cr and V, as shown in Figs. 2(c) and 2(d), indicating the introduction of itinerant carriers. Associated with this carrier doping, however, χ exhibits completely different behaviors between Cr and V; χ at low T is further enhanced for Cr, whereas it is suppressed and approaches a T -independent behavior for V [Figs. 2(a) and 2(b)]. For Cr, the Weiss temperature becomes positive with carrier doping,³ and spontaneous magnetization is observed at very low T (2 K, not shown). These results indicate that (1) itinerant carriers are introduced, presumably into the d band of Ti (nominally Ti^{3+} states) with increasing y for both Cr and V, and (2) they produce ferromagnetic interaction between Cr spins, but antiferromagnetic screening for V.

First, let us see the behavior of the V-doped samples in more detail. One possible scenario for the suppression of χ with carrier doping is that the localized electrons of V^{3+} become itinerant associated with the introduction of itinerant carriers into the Ti d band. If this is the case, the number of carriers for the V-doped sample is larger than that without V. To see this, we performed Hall measurement and compare the result with and without V. As an example, Hall resistivity vs magnetic field for $y=0.1$ and $x=0$ and 0.2 (number of V) is shown in Fig. 3(a). If all the V ion is 3+ for $x=0.2$, then 10% Ti becomes 3+, the same situation as that for $x=0$. Experimental result is such that the slope is smaller for $x=0.2$, indicating that the number of carriers is larger for $x=0.2$ than for $x=0$. We estimated the number of carriers per B site n_c from the Hall coefficient R_H with the relation $R_H = -1/n_c N e c$, where N is the number of the B site per unit volume, and plot the result in Fig. 3(b). The solid line depicts the relation that n_c is the same as y . For $x=0$, the experimental data almost follow the line, indicating that the nominal number of Ti^{3+} (y) really corresponds to the number of itinerant carriers.⁵ However, for $x=0.2$, n_c is discernibly larger than the relation $n_c=y$. This indicates that a part of the electrons on the V ions also become itinerant and contribute to the Hall coefficient.

We also measured the optical reflectivity of the samples with and without V to obtain the information about the effective mass of the itinerant carriers. Comparison between $x=0$ and $x=0.2$ with the same number of y (number of Ti^{3+}) is shown in Figs. 3(c)–3(e). The samples with $x=0$ (without V, shown by the solid lines) exhibit a clear Drude-like behavior with a sharp dip of reflectivity shown by arrows, called a plasma edge, whose frequency corresponds to the plasma frequency ($\hbar\omega_p$). This plasma edge shifts to higher energy with increasing y (carrier concentration in the d band of Ti), consistent with the relations $\omega_p = \sqrt{4\pi n_c e^2/m^*}$, where m^* is the effective mass of carriers, and $n_c=y$. On the other hand, the reflectivity spectrum changes in various aspects with V doping (shown by the dashed lines). First, the plasma edge becomes obscure with V doping, indicating the increase of scattering rate of carriers $1/\tau$. Second, the plasma edge shifts to higher energy with V doping for small y (number of Ti^{3+}), but shifts to lower energy for large y .

To more precisely estimate the value of effective mass from the experiment, we obtained the optical conductivity spectra (shown in the inset of Fig. 3) by the Kramers–Kronig

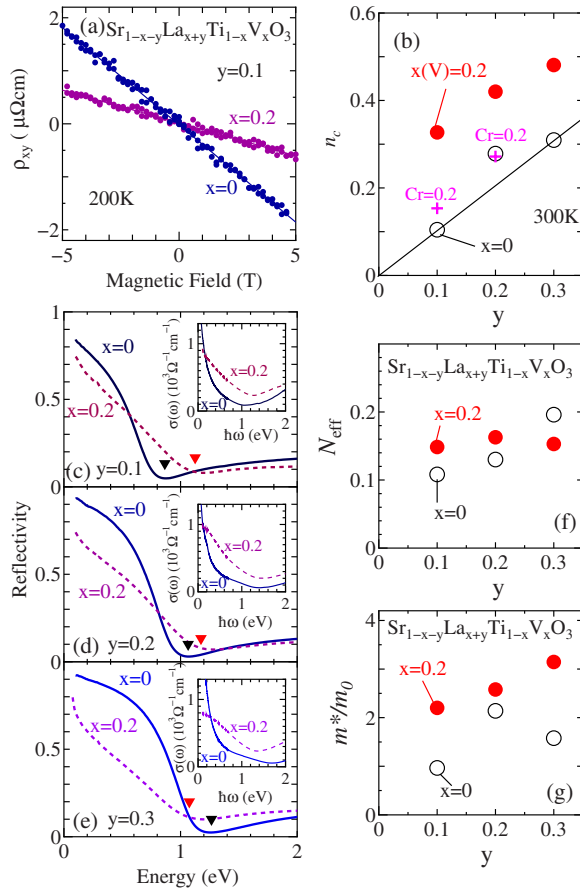


FIG. 3. (Color online) (a) Hall resistivity vs magnetic field for $\text{Sr}_{1-x-y}\text{La}_{x+y}\text{Ti}_{1-x}\text{V}_x\text{O}_3$ with $y=0.1$ (number of Ti^{3+}) and $x=0, 0.2$ (number of V). (b) Carrier concentration n_c estimated from Hall coefficient as a function of y (number of Ti^{3+}) for $\text{Sr}_{1-x-y}\text{La}_{x+y}\text{Ti}_{1-x}\text{V}(\text{Cr})\text{O}_3$ without V or Cr (open circles), with V ($x=0.2$, closed circles), and with Cr (crosses). [(c)–(e)] Optical reflectivity spectra at room temperature for $\text{Sr}_{1-x-y}\text{La}_{x+y}\text{Ti}_{1-x}\text{V}_x\text{O}_3$ with $x=0$ and 0.2 (number of V) and various values of y (number of Ti^{3+}). The insets show the optical conductivity spectrum of each sample. (f) Effective number of electrons (N_{eff}) as a function of y (number of Ti^{3+}) for $\text{Sr}_{1-x-y}\text{La}_{x+y}\text{Ti}_{1-x}\text{V}_x\text{O}_3$ with $x=0$ and 0.2 (number of V). (g) Effective mass m^* normalized to that of free electrons m_0 , estimated from N_{eff} and n_c , as a function of y (number of Ti^{3+}) for $\text{Sr}_{1-x-y}\text{La}_{x+y}\text{Ti}_{1-x}\text{V}_x\text{O}_3$.

transformation of the reflectivity data. We also calculated the effective number of electrons N_{eff} , the integrated value of the optical conductivity below 1.5 eV. As shown in Fig. 3(f), N_{eff} exhibits a seemingly complicated dependence on the V concentration (x) and Ti^{3+} concentration (y), similar to the behaviors of plasma edge. Here, if we assume that all the optical conductivity below 1.5 eV is dominated only by a Drude component for itinerant carriers, N_{eff} equals $n_c/(m^*/m_0)$, where m_0 is the mass of free electrons.⁸ Thus, the effective mass m^* can be calculated from N_{eff} obtained by optical measurement and n_c obtained by Hall measurement. The result is shown in Fig. 3(g), where m^* is simply enhanced with V doping for any y . It should be noted that the optical conductivity below 1.5 eV may not be solely attributed to the Drude spectrum, but may be the sum of a Drude

component and the so-called in-gap state, which is the excitations to localized states,⁹ particularly for the V-doped samples. Since the effective mass calculated from a smaller Drude weight becomes larger, m^* is further enhanced with V doping on this viewpoint.

From these experimental results, the following scenario can be drawn for the V-doped samples. (1) For $y=0$, all the V ions are $3+$ and the d electrons on V^{3+} are localized, i.e., there is a charge gap in the electronic state of V, whereas all the Ti ions are $4+$ and there is no itinerant carriers in the d band of Ti [Fig. 1(b)]. (2) With increasing y , itinerant electrons are introduced to the d band of Ti (Ti^{3+}), and this induces the collapse of the charge gap of V and the electrons on V become also itinerant [Figs. 1(c) and 3(b)]. (3) Since the effective mass of the V electrons is larger than that of the Ti electrons, the average effective mass is also enhanced with V doping [Fig. 3(g)].

Next, let us see the behavior of the Cr-doped samples. As discussed above, electrons on the Cr ion are localized and behave as $S=3/2$ spins for $y=0$. To see how those electrons behave when $y>0$, we measured the Hall coefficient also for the Cr-doped samples. As shown in Fig. 3(b), the variation of n_c with the Cr doping is barely observed, unlike the case of V doping, indicating that the charge gap of Cr survives and the Cr electrons are still localized even with the introduction of itinerant electrons to the Ti $3d$ band [Fig. 1(d)]. It is speculated that different sizes of the Coulomb repulsion energy on V and Cr lead to such different behaviors of the charge gap with the introduction of itinerant carriers. The appearance of ferromagnetic interaction between Cr spins can be attributed to the RKKY-type interaction between Cr localized spins via the itinerant electrons in the Ti $3d$ band, and this yields large negative magnetoresistance reported in Ref. 3.

To further study the electronic properties of the Cr-doped samples at low T , Hall measurement was performed under variation of T . As shown in Fig. 4(a), the slope of Hall resistivity (ρ_{xy}) against magnetic field (H) exhibits a nonlinear behavior below 20 K. This nonlinear behavior can be explained by the anomalous term of Hall resistivity proportional to magnetization, $\rho_{xy} = R_H B + 4\pi R_s M$.¹⁰ We fit the data of ρ_{xy} by this relation with experimentally measured M [the inset of Fig. 2(a)] and R_H and R_s as fitting parameters. The result for the fixed value of $y=0.1$ and various values of x (Cr concentration) is shown in Fig. 4(b). As can be seen, the anomalous term R_s is positive, which is the opposite sign to the normal term R_H , and its absolute value increases with decreasing T . Surprisingly, not only the anomalous term R_s but also the normal term R_H is enhanced with decreasing T . This indicates the reduction of the number of itinerant carriers (n_c) at low T . We calculated the mobility of the carriers, $\mu = R_H/\rho$, and plot it as a function of T , together with ρ itself in Figs. 4(c) and 4(d). As can be seen, μ is almost T independent for all the samples, indicating that the increase of ρ at low T is dominated only by the reduction of n_c . In addition, the absolute value of μ decreases (i.e., the scattering rate $1/\tau$ increases) with increasing Cr concentration.

Such variations of n_c with T , as well as τ with Cr concentration, give us the opportunity to study how the anomalous term R_s depends on n_c and τ . Figure 4(e) shows the relation

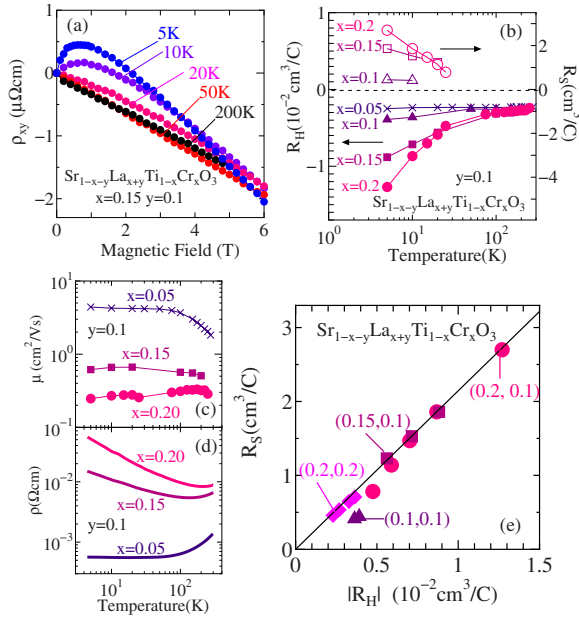


FIG. 4. (Color online) (a) Hall resistivity vs magnetic field for $\text{Sr}_{1-x-y}\text{La}_{x+y}\text{Ti}_{1-x}\text{Cr}_x\text{O}_3$ with $x=0.15$ (number of Cr) and $y=0.1$ (number of Ti^{3+}). (b) Temperature dependence of the normal term R_H (closed symbols, left axis) and the anomalous term R_S (open symbols, right axis) of Hall resistivity for $\text{Sr}_{1-x-y}\text{La}_{x+y}\text{Ti}_{1-x}\text{Cr}_x\text{O}_3$ with $y=0.1$ (number of Ti^{3+}) and various values of x (number of Cr). [(c) and (d)] Temperature dependence of mobility and resistivity for $\text{Sr}_{1-x-y}\text{La}_{x+y}\text{Ti}_{1-x}\text{Cr}_x\text{O}_3$ with $y=0.1$ (number of Ti^{3+}) and various values of x (number of Cr). (e) The anomalous term (R_S) vs the ordinary term (R_H) of Hall resistivity for $\text{Sr}_{1-x-y}\text{La}_{x+y}\text{Ti}_{1-x}\text{Cr}_x\text{O}_3$ with various values of (x, y) .

between R_S and R_H . As can be seen, all the data with different concentrations and different T almost follow a universal line, $R_S = \alpha R_H$ with $\alpha \sim 2 \times 10^2$. This result indicates the following two points: (1) The anomalous term R_S is inversely propor-

tional to the number of itinerant carriers n_c and (2) the difference of mobility for different samples does not largely affect R_S , i.e., R_S barely depends on the relaxation time of itinerant carriers τ .

Hall conductivity σ_{xy} is given by $\sigma_{xy} = \rho_{xy} / \rho^2$. Since ρ is proportional to $1/\tau$, τ -independent R_S as discussed above means τ^2 dependence of anomalous Hall conductivity σ_{xy}^A . A recent theory¹¹ indicates the relation $\sigma_{xy} \propto \tau^{1.6}$ for the ferromagnets in the “intrinsic” regime. The present Cr-doped SrTiO_3 , however, seem to be located not deep into the ferromagnetic phase, but near the quantum critical point between ferromagnetic and paramagnetic phases, since a ferromagnetic phase transition is barely observed or observed only at very low T in this series of compounds. Thus, the present experimental result could be a behavior typical of the system with itinerant carriers and magnetic impurities near the quantum critical point, which might be different from that in the normal ferromagnets.

In summary, we studied the carrier- and magnetic-impurity-doped SrTiO_3 , $\text{Sr}_{1-x-y}\text{La}_{x+y}\text{Ti}_{1-x}\text{V}_x\text{O}_3$ and $\text{Sr}_{1-x-y}\text{La}_{x+y}\text{Ti}_{1-x}\text{V}_x\text{O}_3$. We found that without itinerant carriers in the Ti d band ($y=0$), the electrons on both V and Cr act as localized spins in the system. With carrier doping ($y > 0$), the electrons on V become itinerant with heavy mass, whereas those on Cr remain localized and ferromagnetic interaction appears between them via itinerant electrons in the Ti band. We also found that both the normal term (R_H) and the anomalous term (R_S) of Hall resistivity for Cr-doped samples are enhanced at low temperatures in such a way that $R_S \propto R_H$.

We thank S. Onoda for fruitful discussions. This work was partly supported by a Grant-in-Aid for The 21st Century COE Program at Waseda University and by Grant-in-Aid for Scientific Research on Priority Area, both from MEXT of Japan.

*Author to whom correspondence should be addressed.

¹H. Tsunetsugu, M. Sigrist, and K. Ueda, *Rev. Mod. Phys.* **69**, 809 (1997), and references therein.

²T. Dietl, H. Ohno, F. Matsukura, J. Cibert, and D. Ferrand, *Science* **287**, 1019 (2000), and references therein.

³J. Inaba and T. Katsufuji, *Phys. Rev. B* **72**, 052408 (2005).

⁴H. Iwasawa, K. Yamakawa, T. Saitoh, J. Inaba, T. Katsufuji, M. Higashiguchi, K. Shimada, H. Namatame, and M. Taniguchi, *Phys. Rev. Lett.* **96**, 067203 (2006).

⁵Y. Tokura, Y. Taguchi, Y. Okada, Y. Fujishima, T. Arima, K. Kumagai, and Y. Iye, *Phys. Rev. Lett.* **70**, 2126 (1993).

⁶J. J. Neumeier and H. Terashita, *Phys. Rev. B* **70**, 214435 (2004).

⁷S. Miyasaka, T. Okuda, and Y. Tokura, *Phys. Rev. Lett.* **85**, 5388 (2000).

⁸T. Katsufuji, Y. Okimoto, and Y. Tokura, *Phys. Rev. Lett.* **75**, 3497 (1995).

⁹M. J. Rozenberg, G. Kotliar, H. Kajueter, G. A. Thomas, D. H. Rapkine, J. M. Honig, and P. Metcalf, *Phys. Rev. Lett.* **75**, 105 (1995).

¹⁰W. Lee, S. Watauchi, V. L. Miller, R. J. Cava, and N. P. Ong, *Science* **303**, 1647 (2004), and references therein.

¹¹S. Onoda, N. Sugimoto, and N. Nagaosa, *Phys. Rev. Lett.* **97**, 126602 (2006).